Boundary Layer Flow of Williamson Fluid with Chemically Reactive Species using Scaling Transformation and Homotopy Analysis Method

Najeeb Alam Khan, Sidra Khan and Fatima Riaz*

Department of Mathematical Sciences, University of Karachi, Karachi-75270, Pakistan.

Abstract: The objective of this work is to study the Williamson fluid flow with a chemically reactive species. The governing equations of Williamson model in two dimensional flows are constructed by using scaling transformation under a Reynolds and Weissenberg numbers approximation. The analytic solution of the system of nonlinear ordinary differential equations (ODEs) is constructed in the series form by using homotopy analysis method (HAM). The features of various physical parameters have been discussed graphically on flow and concentration profiles. The result came up with the outcome that the Reynolds number step up the fluid motion but slow down the concentration of the fluid. The Weissenberg number show the distinct effects on the velocity and concentration of the Williamson fluid model.

Keywords: Chemical reaction; Williamson fluid; analytic solution; homotopy analysis method (HAM); similarity transformation.

1 Introduction

The concentration on the effects of chemical reaction in the fluid has been paid to extend the research in literature correspond to the chemical and bio engineering industries. There are many investigations on chemical reaction effects on fluid flow in different physical contexts. Most of the fluids used in daily life have a non-Newtonian behavior. The study of non-Newtonian fluid is important in various fields of sciences such as biomedical engineering, environmental engineering and chemical engineering. Das et al. [1] investigated the effect of mass transfer on flow past an impulsively started infinite vertical plate with constant heat flux and in the presence of chemical reaction. Andersson et al. [2] studied the diffusion of a chemically reactive species from a stretching sheet. The similarity solution of mixed convection flow over a horizontal moving plate with diffusion of chemically reactive species was obtained by Fan et al. [3]. Kandasamy [4] studied the effects of temperature dependent fluid viscosity and chemical reaction on heat and mass transfer with variable stream conditions. The MHD free convection flow and mass transfer over a stretching sheet with chemical reaction

was demonstrated by Afify [5]. Postelnicu [6] showed the influence of chemical reaction on heat and mass transfer by natural convection from vertical surface in porous media with Soret and Dufour effects. Hayat [7] studied the MHD flow and mass transfer of an upper-convected Maxwell fluid past a porous shrinking sheet with chemically reactive species. Bhattacharyya [8] studied the behavior of chemically reactive solute distribution in MHD boundary layer flow over a permeable stretching sheet with suction or blowing.

In recent decades non-Newtonian fluids become more important than Newtonian fluids. Many researchers are working on different non-Newtonian fluid models. Khan [9] investigated the exact analytic solutions for the flow of a generalized Burgers fluid induced by an accelerated shear stress. The Williamson model of non-Newtonian fluid is very much similar to the blood as it almost completely describes the behavior of blood flow due to which it captivated the researcher's attention. The valuable works in this dimension have constantly been added in recent years. Irene and Scarpi [10] obtained the perturbation solution for pulsatile flow of a non-Newtonian Williamson fluid in a rock fracture, Nadeem et al. [11] investigates the effects of heat and

---

* Corresponding author e-mail: njbalam@yahoo.com

mass transfer peristaltic flow of Williamson fluid in a vertical annulus, Vajravelu et al. [12] studied peristaltic transport of a Williamson fluid with permeable walls in asymmetric channel, Hayat et al. [13] found the solution of a Williamson fluid past a porous plate. Akbar et al. [14] calculated the influence of heat transfer and chemical reactions on Williamson fluid model for blood flow through a tapered artery with a stenosis. Investigators also investigate the Peristaltic flow of a Williamson fluid in an inclined asymmetric channel with partial slip and heat transfer [15]. The Analytical and numerical solutions of peristaltic flow of Williamson fluid modeling an endoscope was also obtained by Akbar et al. [16].

In last few years, the flow over a continuous stretching surface is the significant area of study for the investigators, as it has extensive applications in polymer extrusion, manufacturing of glass sheets, chemical engineering plants etc. Crane [17] was the first to consider and examine the boundary layer flow of a viscous fluid over a linearly stretching sheet. Many workers extended his work in different directions. Gupta and Gupta [18] studied the heat and mass transfer in Newtonian boundary layer flow past a stretching sheet with suction and blowing. Lakshmisha [19] studied the three-dimensional unsteady flow with heat and mass transfer over a continuous stretching surface. Wang [20] studied the three-dimensional flow due to a stretching flat surface. Bujurke [21] investigated the Second order fluid flow past a stretching sheet with heat transfer. Sajid [22] studied the Influence of thermal radiation on the boundary layer flow due to an exponentially stretching sheet. Khan [23] studied the effects of slip factors on unsteady stagnation point flow and heat transfer towards a stretching sheet.

Yurusoy and Pakdemirli [24] classified the non-Newtonian fluids on the base of their shear stress, using two different approaches: (1) classical theory and (2) equivalence transformations. Both approaches show us identical results. The Lie group analysis can be found in a simpler way using equivalence transformation. They investigate the special group transformations (i.e. scaling and spiral group transformations), three-dimensional, unsteady, boundary layer equations of non-Newtonian fluids. Yurusoy et al. [25] obtained the Lie group analysis of creeping flow of a second grade fluid.

In this paper, our aim is to study the Williamson fluid flow with a chemically reactive species. Using scaling transformation technique viz., Lie group transformations. Using the symmetry our governing partial differential equations transformed into nonlinear ordinary differential equations. The scaling symmetry is well known to exist for boundary layer type problems leading to useful solutions and for this reason, the specific form of the scaling symmetry which leaves the equations invariant is determined [26-28]. The transformed equations are solved and analyzed with the help of homotopy analysis method (HAM).

2 Problem Formulation

The theory of rate processes is used to drive the Williamson fluid model for describing the shear of a non-Newtonian flow. In some cases this model predicts the viscous behavior of polymer solutions and viscoelastic suspension over a wide range of shear rates. For an incompressible fluid, the balance of mass and momentum are given by

$$\text{Div}\mathbf{V} = 0, \tag{1}$$

$$\rho\frac{d\mathbf{V}}{dt} = \text{Div}\mathbf{S} + \rho f, \tag{2}$$

Where ρ is the density, $\mathbf{V}$ is the velocity vector, $\mathbf{S}$ is the Cauchy stress tensor, f represents the specific body force and $\frac{d}{dt}$ represents the material time derivative. The Cauchy stress tensor for Williamson fluid is given by

$$\mathbf{S} = -p\mathbf{I} + \mathbf{T}, \tag{3}$$

$$\mathbf{T} = [\mu_\infty + (\mu_0 - \mu_\infty)(1 - \Gamma|\bar{\bar{\gamma}}|)^{-1}]\bar{\bar{\gamma}} \tag{4}$$

In which $p\mathbf{I}$ is the spherical part of the stress due to constraint of incompressibility, $\mathbf{T}$ is the extra stress tensor, μ_∞ is the infinite shear rate viscosity, μ_0 is the zero shear rate viscosity, Γ is the time constant and $\bar{\bar{\gamma}}$ is defined as,

$$|\bar{\bar{\gamma}}| = \sqrt{\frac{1}{2}\sum_i\sum_j\overline{\dot{\gamma}_{ij}}\,\overline{\dot{\gamma}_{ji}}} = \sqrt{\frac{1}{2}\Pi} \tag{5}$$

The Π is the second invariant strain tensor. We consider the Eq. (4), the case for which $\mu_\infty = 0$ and $\Gamma\bar{\bar{\gamma}} < 1$. The component of extra stress tensor therefore, can be written as

$$\mathbf{t} = [\mu_0(1 - \Gamma|\bar{\bar{\gamma}}|)^{-1}]\bar{\bar{\gamma}} \tag{6}$$

Steady-state, two dimensional, incompressible equations of motion including mass conservation can be written as

$$\frac{\partial\bar{u}}{\partial\bar{x}} + \frac{\partial\bar{v}}{\partial\bar{y}} = 0 \tag{7}$$

$$\rho\left(\bar{u}\frac{\partial\bar{u}}{\partial\bar{x}} + \bar{v}\frac{\partial\bar{u}}{\partial\bar{y}}\right) = -\frac{\partial\bar{p}}{\partial\bar{x}} + \frac{\partial\tau_{xx}}{\partial\bar{x}} + \frac{\partial\tau_{xy}}{\partial\bar{y}} \tag{8}$$

$$\rho\left(\bar{u}\frac{\partial\bar{v}}{\partial\bar{x}} + \bar{v}\frac{\partial\bar{v}}{\partial\bar{y}}\right) = -\frac{\partial\bar{p}}{\partial\bar{y}} + \frac{\partial\tau_{yx}}{\partial\bar{x}} + \frac{\partial\tau_{yy}}{\partial\bar{y}} \tag{9}$$

$$\overline{u}\frac{\partial \overline{C}}{\partial \overline{x}} + \overline{v}\frac{\partial \overline{C}}{\partial \overline{y}} = D(\frac{\partial^2 \overline{C}}{\partial \overline{x}^2} + \frac{\partial^2 \overline{C}}{\partial \overline{y}^2}) \tag{10}$$

Where $\overline{x}$ is the spatial coordinate along the surface, $\overline{y}$ is vertical to it $\overline{u}$ and $\overline{v}$ are the velocity components in the $\overline{x}$ and $\overline{y}$ coordinates, $\overline{C}$ is the concentration, D is the diffusion coefficient. The shear stress components are inserted into the equations of motion and the usual boundary layer assumptions are made i.e. the highest order terms are retained and momentum equations become

$$\rho(\overline{u}\frac{\partial \overline{u}}{\partial \overline{x}} + \overline{v}\frac{\partial \overline{u}}{\partial \overline{y}}) = -\frac{\partial \overline{p}}{\partial \overline{x}} + \mu_0\frac{\partial^2 \overline{u}}{\partial \overline{y}^2} + \mu_0\frac{\partial \overline{u}}{\partial \overline{y}}\frac{\partial^2 \overline{u}}{\partial \overline{y}^2} \tag{11}$$

$$\frac{\partial \overline{p}}{\partial \overline{y}} = 0 \tag{12}$$

$$\overline{u}\frac{\partial \overline{C}}{\partial \overline{x}} + \overline{v}\frac{\partial \overline{C}}{\partial \overline{y}} = D\frac{\partial^2 \overline{C}}{\partial \overline{y}^2} \tag{13}$$

The Eqs. (11)-(12) shows that the pressure on $\overline{y}$ is eliminated. The dimensional variables are given as:

$$x = \frac{\overline{x}}{L}, y = \frac{\overline{y}}{L}, u = \frac{\overline{u}}{V}, v = \frac{\overline{v}}{V}, p = \frac{\overline{p}}{\rho V^2}, C = \frac{\overline{C}}{C_w}, Re = \frac{LV\rho}{\mu_0}, We = \frac{\Gamma V}{L}, \gamma = \frac{D}{LV} \tag{14}$$

Where L is a length, V is a velocity, C_w denotes the concentration at the stretching sheet. We is a Weissenberg number and Re is a Reynolds number. By using the above non-dimensionless parameters in Eqs. (7), (11), (13) which lead to the equations:

$$\frac{\partial u}{\partial x} + \frac{\partial v}{\partial y} = 0 \tag{15}$$

$$\rho(u\frac{\partial u}{\partial x} + v\frac{\partial u}{\partial y}) = -\frac{\partial p}{\partial x} + \frac{1}{Re}\frac{\partial^2 u}{\partial y^2} + 2\frac{We}{Re}\frac{\partial u}{\partial y}\frac{\partial^2 u}{\partial y^2} \tag{16}$$

$$u\frac{\partial C}{\partial x} + v\frac{\partial C}{\partial y} = \gamma\frac{\partial^2 C}{\partial y^2} \tag{17}$$

The classical boundary conditions for the problem are

$$u(x,0) = 0, v(x,0) = 0, u(x,\infty) = U(x), C(x,0) = 1, C(x,\infty) = 0 \tag{18}$$

For $We = 0$, the Eqs. (15)-(17) reduce to those of Newtonian fluid.

3 Scaling Transformations

Now, introducing the simplified form of Lie-group transformations, namely the scaling group of transformation as:

$$x^* = \xi^a x, y^* = \xi^b y, u^* = \xi^c u, v^* = \xi^d v, U^* = \xi^e U, C^* = \xi^j C, \tag{19}$$

Substituting Eq. (19) into Eqs. (15)-(17) and requiring that the equations be invariant under the transformation yields

$$b + c - a - d = 0, 2c - 2e = 0, a - 3b = 0, 4b - c - a = 0 \tag{20}$$

All parameters are solved in terms of parameter b

$$a = 3b, c = b, d = -b, e = b, j = 0 \tag{21}$$

The associated equations for this transformation which define similarity variables are

$$\frac{dx}{3x} = \frac{dy}{y} = \frac{du}{u} = \frac{dv}{-v} = \frac{dU}{U} = \frac{dC}{C} \tag{22}$$

The similarity variables and functions are

$$\eta = \frac{y}{x^{1/3}}, u = x^{1/3}f(\eta), v = \frac{g(\eta)}{x^{1/3}}, U = x^{1/3}, C = \phi(\eta) \tag{23}$$

Substituting all these values of Eq. (23) into the boundary layer equations Eqs. (15)-(17) yields the ordinary differential equations

$$3g' - \eta f' + f = 0 \tag{24}$$

$$\frac{3}{Re}f'' + 6\frac{We}{Re}f'f'' + \eta ff' - 3gf' - f^2 + 1 = 0 \tag{25}$$

$$3\gamma\phi'' - 3g\phi' + \eta f\phi' = 0 \tag{26}$$

The boundary conditions in Eq. (18) reduce to

$$f(0) = 0, f(\infty) = 1, g(0) = 0, \phi(0) = 1, \phi(\infty) = 0, \tag{27}$$

4 Solution of the problem

For the two dimensional problem presented in Eqs. (24)-(26), the course of action for the HAM solution, we select

$$f_0 = 1 - e^{-\eta}, g_0 = 0, \phi_0 = e^{-\eta}, \tag{28}$$

The initial approximation of f_0, g_0 and ϕ_0 in Eq. (28), satisfy the following linear operator and their boundary conditions

$$L_1 = \frac{d}{d\eta} + 1, L_2 = \frac{d^2}{d\eta^2} + \frac{d}{d\eta}, L_3 = \frac{d^2}{d\eta^2} - 1, \quad (29)$$

such that

$$L_1 = [c_1 e^{-\eta}] = 0, L_2 = [c_2 e^{-\eta} + c_3] = 0, L_3 = [c_4 e^{\eta} + c_5 e^{-\eta}] = 0, \quad (30)$$

where $c_1, c_2, ..., c_5$ are arbitrary constants.
The following nonlinear operators are defined as:

$$N_1[\widetilde{f}(\eta, p), \widetilde{g}(\eta, p)] = 3\frac{\partial \widetilde{g}(\eta, p)}{\partial \eta} - \eta \frac{\partial \widetilde{f}(\eta, p)}{\partial \eta} + \widetilde{f}(\eta, p) \quad (31)$$

$$N_2[\widetilde{f}(\eta, p), \widetilde{g}(\eta, p)] = \frac{3}{Re} \frac{\partial^2 \widetilde{f}(\eta, p)}{\partial \eta^2}$$
$$+ 6\frac{We}{Re} \frac{\partial \widetilde{f}(\eta, p)}{\partial \eta} \frac{\partial^2 \widetilde{f}(\eta, p)}{\partial \eta^2} + \eta \widetilde{f}(\eta, p) \frac{\partial \widetilde{f}(\eta, p)}{\partial \eta}$$
$$- 3\widetilde{g}(\eta, p)\frac{\partial \widetilde{f}(\eta, p)}{\partial \eta} - (\widetilde{f}(\eta, p))^2 + 1 \quad (32)$$

$$N_3[\widetilde{f}(\eta, p), \widetilde{g}(\eta, p), \widetilde{\phi}(\eta, p)] = 3\gamma\frac{\partial^2 \widetilde{\phi}(\eta, p)}{\partial \eta^2}$$
$$- 3\widetilde{g}(\eta, p)\frac{\partial \widetilde{\phi}(\eta, p)}{\partial \eta} + \eta \widetilde{f}(\eta, p)\frac{\partial \widetilde{\phi}(\eta, p)}{\partial \eta} \quad (33)$$

and then construct the *zeroth* order deformation equations

$$(1 - p)L_1[\widetilde{g}(\eta, p) - g_0] - p\hbar N_1[\widetilde{f}(\eta, p), \widetilde{g}(\eta, p)] = 0 \quad (34)$$

$$(1 - p)L_2[\widetilde{f}(\eta, p) - f_0] - p\hbar N_2[\widetilde{f}(\eta, p), \widetilde{g}(\eta, p)] = 0 \quad (35)$$

$$(1 - p)L_3[\widetilde{\phi}(\eta, p) - \phi_0] - p\hbar N_3[\widetilde{f}(\eta, p), \widetilde{g}(\eta, p), \widetilde{\phi}(\eta, p)] = 0$$

$$\widetilde{g}(0, p) = 0, \widetilde{f}(0, p) = 0, \widetilde{f}(\infty, p) = 1, \widetilde{\phi}(\infty, p) = 0, \widetilde{\phi}(0, p) = 1,$$

In which $p \in [0, 1]$ is the embedding parameter and is the auxiliary non zero parameter.

$$\widetilde{f}(\eta, p) = f_0(\eta) + \sum_{i=0}^{m-1} f_m(\eta)p^m,$$

$$\widetilde{g}(\eta, p) = g_0(\eta) + \sum_{i=0}^{m-1} g_m(\eta)p^m,$$

$$\widetilde{\phi}(\eta, p) = \phi_0(\eta) + \sum_{i=0}^{m-1} \phi_m(\eta)p^m \quad (36)$$

The *mth* order deformation problems with the corresponding boundary conditions are given by

$$L_1[g_m - \chi_m g_{m-1}] = \hbar R_1[f_{m-1}, g_{m-1}] \quad (37)$$

$$L_2[f_m - \chi_m f_{m-1}] = \hbar R_2[f_{m-1}, g_{m-1}] \quad (38)$$

$$L_3[\phi_m - \chi_m \phi_{m-1}] = \hbar R_3[f_{m-1}, g_{m-1}, \phi_{m-1}] \quad (39)$$

$$g_m(0) = 0, f_m(0) = 0, f_m(\infty) = 0, \phi_m(0) = 0, \phi_m(\infty) = 0, \quad (40)$$

where

$$R_1[f_{m-1}, g_{m-1}] = 3g'_{m-1} - \eta f'_{m-1} + f_{m-1} \quad (41)$$

$$R_2[f_{m-1}, g_{m-1}] = \frac{3}{Re}f''_{m-1} + 6\frac{We}{Re}\sum_{i=0}^{m-1} f'_i f''_{m-1-i}$$
$$+ \eta \sum_{i=0}^{m-1} f_i f'_{m-1-i} - 3\sum_{i=0}^{m-1} g_i f'_{m-1-i}$$
$$- \sum_{i=0}^{m-1} f_i f_{m-1-i} + (1 - \chi_m) \quad (42)$$

$$R_3[f_{m-1}, g_{m-1}, \phi_{m-1}] = 3\gamma\phi''_{m-1} - 3\sum_{i=0}^{m-1} g_i\phi'_{m-1-i} + \eta\sum_{i=0}^{m-1} f_i\phi'_{m-1-i} \quad (43)$$

where

$$\chi_m = \begin{cases} 0, & m \leq 1 \\ 1, & m \geq 2 \end{cases}$$

According to the process defined above, it is easy to solve the linear Eqs. (39)-(41), one after the other in the order m, especially by means of any computation software, such as MATHEMATICA.

5 Results and Discussions

The numerical computations are performed for various values of physical parameters involved in the Eqs. (31)-(33). The Reynolds number Re, Weissenberg number We and the reaction rate parameter γ have been encountered in this problem.

In Fig. 1 and Fig. 2, f function is related to the horizontal-component of the velocity. Fig. 1 shows the changes on function f at different values of Reynolds number. The boundary layer becomes thicker when increase the values of Reynolds number. Fig. 2 also shows the similar behavior. But when we increase the
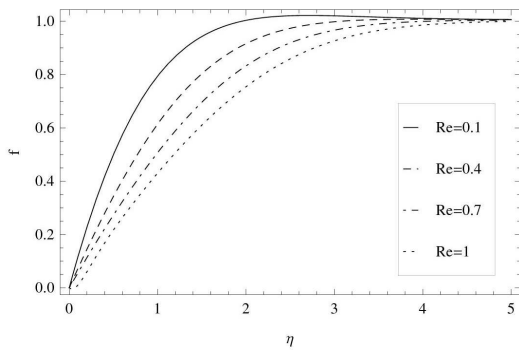
Fig. 1: The velocity profiles $f(\eta)$ for various values of Re ($We = 2$)
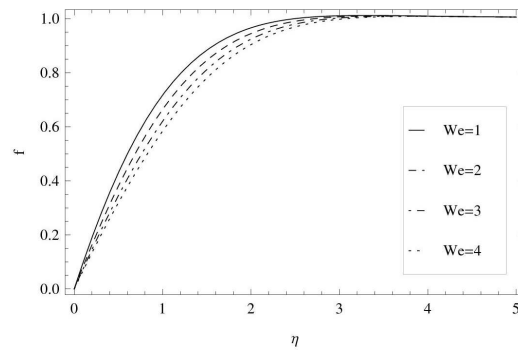
Fig. 2: The velocity profiles $f(\eta)$ for various values of We ($Re = 0.3$)

Weissenberg number, the change in boundary layer thickness is minute as compare to Fig. 1.

In Fig. 3 and Fig. 4, function g is related to the vertical-component of velocity. From Fig. 3 we observed that the increase in the values of Reynolds number also increases the vertical-component of velocity in domain. Similarly Fig. 4 shows that an increase in Weissenberg number give rise to the vertical-component of velocity in domain, but this increase is minute as compare to the Fig. 3.

Fig. (5)-(7), shows the variation of concentration profiles for various values of γ, Re and We The concentration profiles for different values of γ keeping Re and We constantan can be observed from Fig. 5, an increase in γ increasees the boundary layer thickness of concentration profiles. Fig. 6, shows that the an increase in Re decreases the boundary layer thickness of concentration profiles. Similarly Fig. 7 shows the same behavior as compare to the Fig. 6. It is also evident of the decrease in the boundary layer thickness. Re and We both show the decrease in concentration profile because they both are not directly involved in the Eq. (26).

For the solution of Williamson fluid model with chemical reaction and to certify the convergence of the series solutions, the most suitable value of $\hbar$ is required. Fig. 8 shows that the velocity profiles $f(\eta)$ converges at $-0.3 < \hbar < 0.4$. Fig. 9 expresses the velocity profiles $g(\eta)$ converges at $-0.1 < \hbar < 0.3$. Fig. 10 displays the concentration profiles $\phi(\eta)$ converges at $-0.1 < \hbar < 0.3$.

Fig. 3: The velocity profiles $g(\eta)$ for various values of Re ($We = 2$)

Fig. 4: The velocity profiles $g(\eta)$ for various values of We ($Re = 0.3$)

6 Conclusions

The present paper is modeled the chemically reacting Williamson fluid flow over a stretching sheet. The governing equations are transformed to ordinary differential equations with the help of scaling
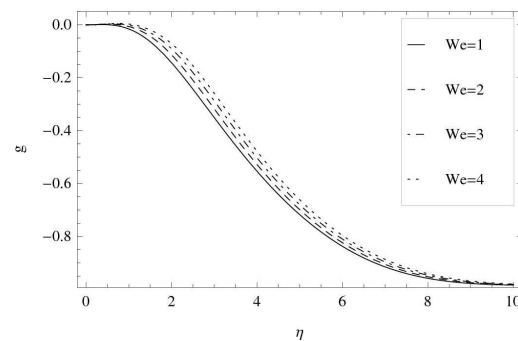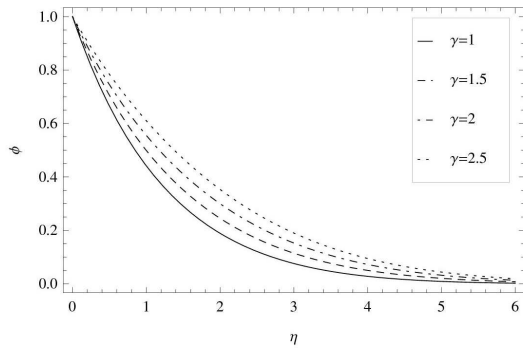
Fig. 5: Concentration profiles $\phi(\eta)$ for various values of γ ($Re = 0.1, We = 1$)
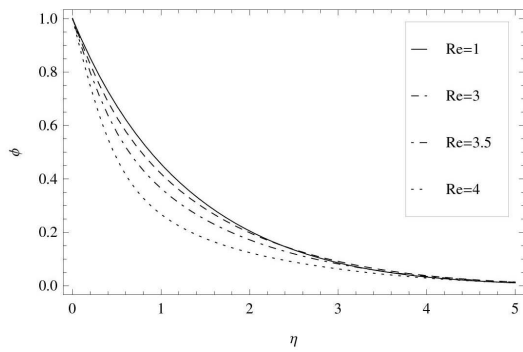
Fig. 6: Concentration profiles $\phi(\eta)$ for various values of Re ($\gamma = 1, We = 2$)
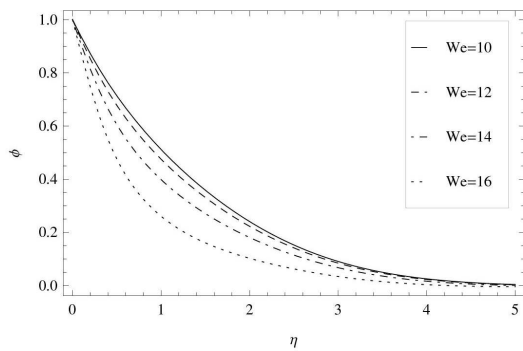
Fig. 7: Concentration profiles $\phi(\eta)$ for various values of We ($Re = 0.3, \gamma = 1$)
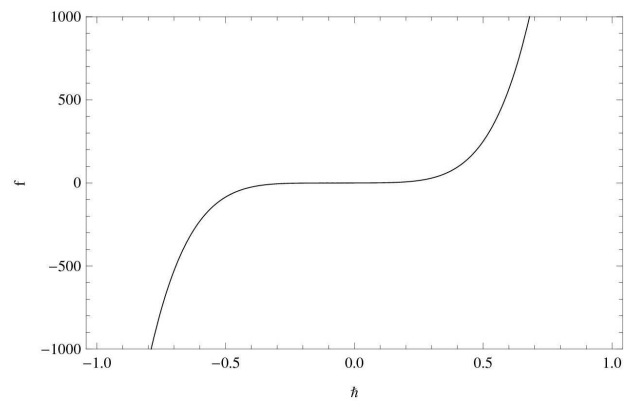
Fig. 8: The $\hbar$ curves for the velocity profiles $f(\eta)$
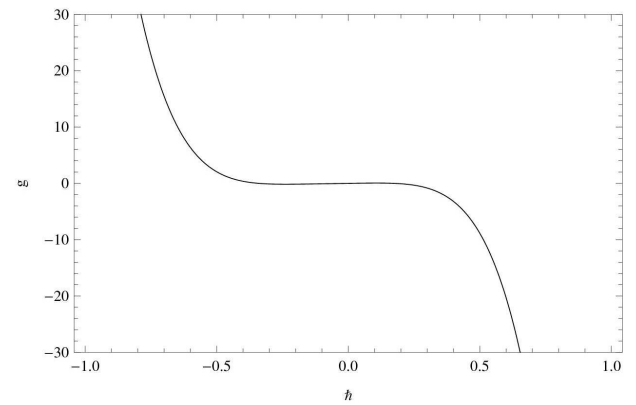
Fig. 9: The $\hbar$ curves for the velocity profiles $g(\eta)$
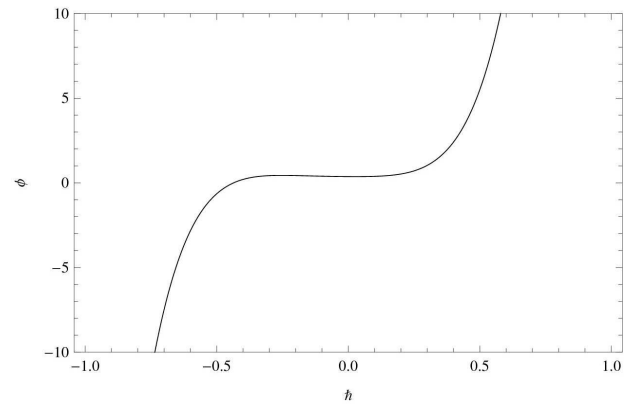
Fig. 10: The $\hbar$ curves for the velocity profiles $\phi(\eta)$

transformation. The homotopy analysis method has been employed to obtain the analytical solution of the governing problem. The influences of the pertinent parameters are investigated on the velocity and concentration. The investigation came up with the following results.

• The Reynolds number accelerates the fluid motion but decelerates the concentration of the Williamson fluid.

• The Weissenberg number has the diverse effects on the velocity and concentration of the fluid as it decreases the horizontal component of velocity $f(\eta)$ and increases the vertical velocity function $g(\eta)$ and concentration function $\phi(\eta)$.

• The concentration of the fluid is enhanced due to reaction rate parameter γ.

References

[1] U.N. Das, R.K. Deka, V.M. Soundalgekar, Forsch. Ingenieurwes **60**, 284-287 (1994).

[2] H.I. Andersson, O.R. Hansen, B. Holmedal, International Journal of Heat and Mass Transfer **37**(4), 659-664 (1994).

[3] J.R. Fan, J.M. Shi, X.Z. Xu, Acta Mechanica **126**, 59-69 (1998).

[4] R. Kandasamy, M. Ismoen, H.B. Saim, Nuclear Engineering and Design **240**, 39-46 (2010).

[5] A. Afify, International Journal of Heat and Mass Transfer **40**, 495-500 (2004).

[6] A. Postelnicu, International Journal of Heat and Mass Transfer **43**(6), 595-602 (2007).

[7] T. Hayat, Z. Abbas, N. Ali, Physics Letters A **372**(26), 4698-4704 (2008).

[8] K. Bhattacharyya, G.C. Layek, Chemical Engineering Communications **197**, 1527-1540 (2010).

[9] M. Jamil, A.A. Zafar, C. Fetecau, N. A. Khan, Chemical Engineering Communications **199**, 17-39 (2012).

[10] D. Irene, S. Giambattista, International Journal of Rock Mechanics and Mining Sciences **44**, 271-278 (2007).

[11] S. Nadeem, N.S. Akbar, Meccanica **47**(1), 141-151 (2012).

[12] K. Vajravelu, S. Sreenadh, K. Rajanikanth, C. Lee, Nonlinear Analysis: Real World Applications **13**(6), 2804-2822 (2012).

[13] T. Hayat, U. Khalid, M. Qasim, Asia-Pacific Journal of Chemical Engineering **7**(2), 302-306 (2012).

[14] N.S. Akbar, S. Nadeem, C. Lee, Asian Journal of Chemistry **24**, 2433-2441 (2012).

[15] N.S Akbar, T. Hayat, S. Nadeem, S. Obaidat, International Journal of Heat and Mass Transfer **55**, 1855-1862 (2012).

[16] N.S Akbar, S. Nadeem, Journal of Mechanics in Medicine and Biology **11**(1), 941-957 (2011).

[17] L. Crane, ZAMP **21**, 645-647 (1970).

[18] P.S. Gupta and A.S. Gupta, Canadian Journal of Chemical Engineering **55**, 744-746 (1977).

[19] K.N. Lakshmisha, S. Venkateswaran, G. Nath, ASME Journal of Heat Transfer **110**, 590-595 (1988).

[20] C.Y. Wang, Physics of Fluids, **27**, 1915-1917 (1984).

[21] N.M. Bujurke, S.N. Biradar, P.S. Hiremath, ZAMP **38**, 653-657 (1987).

[22] M. Sajid, T. Hayat, International Communications in Heat and Mass Transfer **35**(3), 347-356 (2008).

[23] N.A. Khan, M. Jamil, N.A. Khan, Heat Transfer Research **43**(8), 779-794 (2012).

[24] M. Yurusoy, M. Pakdemirli, International Journal of Non-Linear Mechanics **34**, 341-346 (1999).

[25] M. Yurusoy, M. Pakdemirli, International Journal of Non-Linear Mechanics **36**, 955-960 (2001).

[26] M. Pakdemirli, International Journal of Non-Linear Mechanics **27**, 785-793 (1992).

[27] M. Pakdemirli, IMA Journal of Applied Mathematics **50**, 133-148 (1993).

[28] M. Pakdemirli, International Journal of Engineering Science **32**, 141-154 (1994).